Oblique incidence of semi-guided waves on step-like folds in planar dielectric slabs: Lossless vertical interconnects in 3-D integrated photonic circuits

Andre Hildebrandt, Samer Alhaddad, Manfred Hammer, and Jens Förstner

Institute of Electrical Engineering, Paderborn University,
Warburger Strasse 100, D-33098 Paderborn, Germany

ABSTRACT

Semi-guided light propagation across linear folds of slab waveguides is being considered. Radiation losses vanish beyond certain critical angles of incidence, as can be understood by arguments resembling Snell's law. One thus realizes lossless propagation through 90-degree corner configurations, where the remaining guided waves are still subject to pronounced reflection and polarization conversion. A step-like system of two of these sharp corners can then be viewed as a system akin to a Fabry-Perot interferometer, with two partial reflectors at a distance given by the vertical separation of the slab cores. The respective resonance effect enables full transmission of semi-guided, laterally plane waves through the step structures. One obtains a configuration that optically connects guiding layers at different elevation levels in a 3-D integrated optical chip, without radiation losses, over large distances, and reasonably broadband. We show rigorous quasi-analytical results for typical high-contrast Si/SiO_2 structures. Although the full-transmission effect requires a symmetric system, here realized by slab waveguides with a silicon core sandwiched between thick silica substrate and cover layers, simulations for configurations with air cover show that a certain asymmetry can well be afforded.

Keywords: integrated optics, slab waveguide discontinuities, thin-film transitions, 90-degree waveguide corners, vertical couplers, numerical / analytical modeling, silicon photonics

1. INTRODUCTION

Silicon has been the dominating material platform of microelectronics over half a century. Continuous technological advances in circuit design and manufacturing make it possible for quite some time now, to combine electronic and photonic devices on the same platform, further increasing the performance and decreasing the consumed energy.[1] Since photonic devices tend to be rather large compared to electronic ones, concepts for 3-D integration with compact, high-contrast dielectric optical waveguides at different levels of photonic chips have been proposed.[2,3] These concepts include small vertical distances, where an evanescent coupling between overlapping components is possible, but also large vertical distances, where the waveguides are optically separated. Particularly in the latter case the question arises, how the power over these vertical distances can be transfered, for conventional evanescent couplers lead either to large devices in centimeter scale[4] or to shorter devices with vertical distances up to only a few tens of nanometers.[5] Other concepts for vertical power transfer use the coupling of waveguides with specifically tapered cores,[6,7] radiative coupling through grating couplers[8] or resonant interaction of vertically stacked microrings.[9] To our knowledge the drawback of all concepts are either the requirement of large space, high power losses, or their complexity. In this paper a step-like structure, as sketched in Fig. 1(b), is investigated, which needs less space than other concepts, while exhibiting full transmission to arbitrary vertical distances. It continues the theoretical approach discussed in Refs. [10, 11], extending it to air claddings.

Consider the step configuration of Fig. 1(b), consisting of two 90° corners like in (a) that connects half-infinite film waveguides at different elevation levels. The entire structure is assumed to be constant along the y-direction, leading to a two-dimensional problem. We assume parameters for film waveguides with a silicon core grown on a silicon dioxide substrate (or thick buffer layer), with alternatively oxide or air cover. The incoming guided

Send correspondence to andre.hildebrandt@uni-paderborn.de

slab mode propagates in the y-z plane. At normal incidence of the fundamental TE slab mode, for $\theta = 0°$, such a step exhibits a transmittance of merely $T = 3\%$ and a reflectance of $R = 11\%$. Most of the power is lost to radiation and, moreover, gives a potential of unwanted cross talk. However, if the in-plane angle of incidence is set to a specific value, one obtains, with the same vertical step, transmittances of $T > 99\%$, where all radiation losses are prohibited.

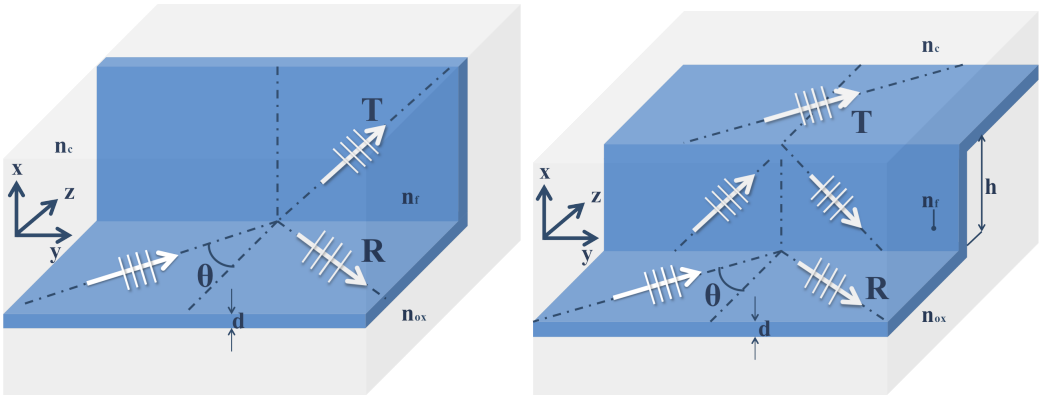

(a) (b)

Figure 1: Sketch of (a) the corner and (b) the step configuration. Parameters: $n_f = 3.45$ (slab core), $n_{ox} = 1.45$ (substrate) and $n_c = 1.45$ or $n_c = 1$ (depending on the cladding); slab thickness $d = 220$ nm; vacuum wavelength $\lambda_0 = 1.55$ μm

In the following both, the symmetrical and asymmetrical case, where the waveguide is covered with silicon dioxide or left bare, are investigated. In section 2 we look at single 90° corners first. In section 3 a Fabry-Perot model is introduced, which explains the fundamental resonance mechanism of the step structures. Section 4 then discusses simulation results for the entire step configurations, showing full transmission and the necessary resonance conditions.

For all simulations in this paper a rigorous, semi-analytical solver (vectorial quadridirectional eigenmode propagation, vQUEP)[12–14] has been used to solve the vectorial 2D problems.

2. SLAB WAVEGUIDES WITH VERTICAL CORNERS AT OBLIQUE INCIDENCE

Starting point is a single corner as sketched in 1 (a). We assume that the waveguide is single mode, supporting only the fundamental guided TE_0 and TM_0 mode, with the effective mode indices N_{TE_0} and N_{TM_0}, for the vacuum wave number of k_0, where $N_{TE_0} > N_{TM_0}$. The TE_0 mode is supposed to come in at the corner under an angle of incidence of θ. Then, besides any radiated, non-guided fields, one expects some transmitted guided waves that propagate upwards, guided by the vertical slab, and a reflected guided part that remains in the x-y-plane. For non-perpendicular incidence $\theta \neq 0$, the outgoing guided waves can include both the TE_0 and TM_0 modes, where the outgoing modes are observed each at its own specific angle θ_{out}.

The structure is constant along the y-direction. The incoming field exhibits an exponential dependence $\sim \exp(-ik_y y)$ with a wavenumber $k_y = k_0 N_{TE0} \sin\theta$, given by the angle of incidence. Therefore, aiming at a solution of the homogeneous Maxwell equations in the frequency domain, we may restrict the y-dependence of all fields to this single spatial Fourier component given by the incident field. The incoming and all transmitted and reflected waves share this y-dependence, which leads to an expression in the form of Snell's law:

$$N_{out} \sin\theta_{out} = N_{TE0} \sin\theta. \tag{1}$$

Variants of Snell' law have been known for slab waveguides with straight discontinuities, typically end facets, with oblique incidence of guided modes,[15–18] and for slab waveguides with periodic corrugations at oblique incidence.[19,20] In the present context, we've shown it to be applicable to vertical corners (or, in fact, to generalized "discontinuities" with slab waveguides at quite arbitrary angles), as well.[10,11]

For an outgoing mode with small effective index N_{out}, or more specifically, if $k_0^2 N_{out}^2 < k_y^2$, equation (1) does not apply and the outgoing field becomes evanescent. That means for this configuration, that the TM_0 mode does not carry power to the far field, if the TE_0 mode comes in at an angle $\theta > \theta_{TM}$, beyond a critical angle θ_{TM} given by the ratio $\sin\theta_{TM} = N_{TM0}/N_{TE0}$. Note that the TM_0 mode still contributes to the total field close to the corner, even for $\theta > \theta_{TM}$.

Apart from the two guided modes, a continuum of unguided modes, the so called substrate and cladding modes, can be associated with the horizontal and vertical slabs. With a similar argumentation one predicts other critical angles θ_{ox}, with $\sin\theta_{ox} = n_{ox}/N_{TE_0}$, for the oxide substrate and / or cladding, and θ_{air}, with $\sin\theta_{air} = n_{air}/N_{TE_0}$, for the air cover. For incidence of the TE_0 mode at angles larger than θ_{ox} and θ_{air}, any radiation into the oxide or air cladding, respectively, is suppressed. Note that, due to different effective indices N_{TE}, the critical angles for case (a) differ from those for (b) and (c).

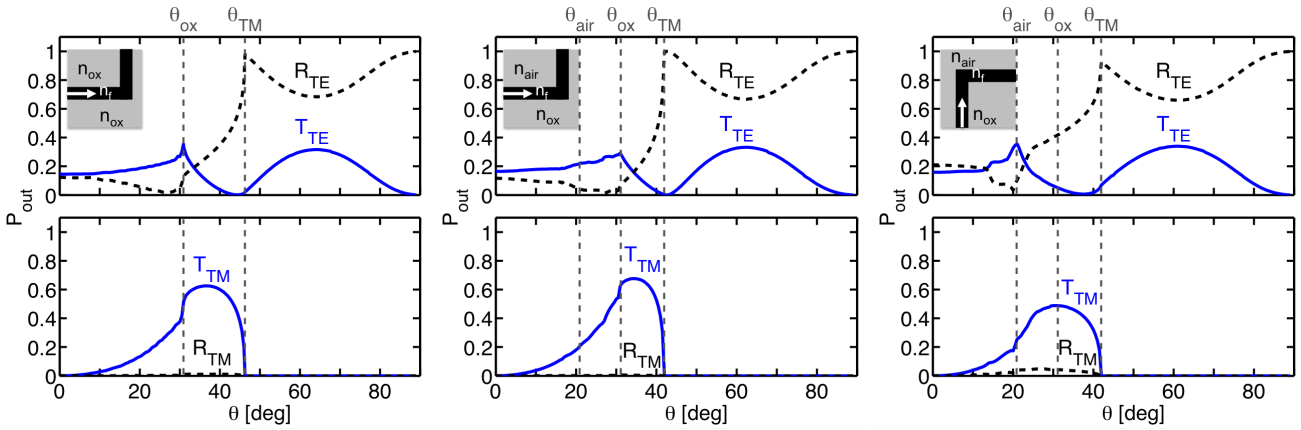

(a) (b) (c)

Figure 2: Modal transmittances T_{TE} and T_{TM} and reflectances R_{TE} and R_{TM} depending on the angle of incidence θ. The critical angles θ_{air}, θ_{ox}, and θ_{TM} are indicated by dashed lines. Shown are the symmetrical case in (a) and the asymmetrical case for two different configurations in (b) and (c), indicated by the insets.

In Fig. 2 one can see the power transmission properties of three corner structures, concerning the fundamental guided modes, as a function of the angle of incidence. At normal incidence $\theta = 0°$, the otherwise vectorial equations split into the standard scalar 2D Helmholtz problem, thus no polarization conversion can be observed. The differences between the symmetrical case (a, oxide substrate and cladding) and the asymmetrical cases (b, c, air cover) become mainly apparent for incidence angles below the critical angle θ_{TM}. It is apparent that the critical angle for the material "straight ahead" (i.e. θ_{ox} for configuration (b), θ_{air} for configuration (c)) is the most relevant, what concerns the diminishing radiation. Strict comparison of the curves shows that the transmittance of the two asymmetric corner configurations differs slightly, also for $\theta > \theta_{TM}$. The significance of that is investigated in the next section.

In Fig. 3 the normalized absolute values $|\mathbf{E}|$ of the electric field for different angles of incidence are shown for the case that the structure is not clad. For normal incidence in (a) most of the field radiates into the substrate. In (b) the angle $\theta = 24°$ lies between the critical angles θ_{air} and θ_{ox}. Here any radiation into the air region is suppressed, radiation occurs only into the oxide region. Radiative losses are completely suppressed for $\theta > \theta_{ox}$ and in (c) and (d).

3. FABRY-PEROT MODEL FOR STEP-DISCONTINUITIES

After having discussed a single corner configuration it is only logical to extend this system to a step-discontinuity as sketched in Fig. 1(b). Before this system is calculated fully, a more simple picture is introduced. As long as the incident angle θ is greater than the critical angles θ_{ox} and θ_{air}, the whole energy remains guided, i.e. there cannot occur any radiation losses. For the case, that the film is surrounded homogeneously with the same

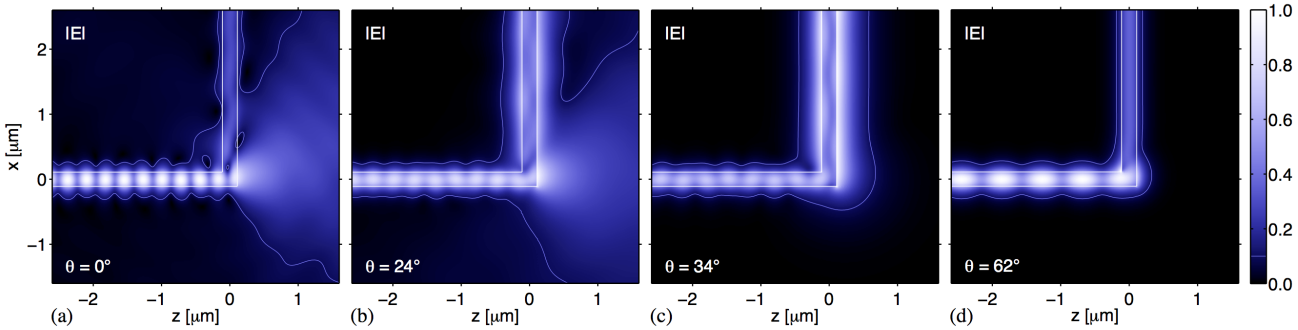

Figure 3: Field profile (normalized absolute value $|\mathbf{E}|$ of the electric field, contour at 10% of the field maximum) for the angles of incidence (a) $\theta = 0°$, (b) $\theta = 24°$, (c) $\theta = 34°$, and (d) $\theta = 62°$; configuration with air cladding, Fig. 1(b).

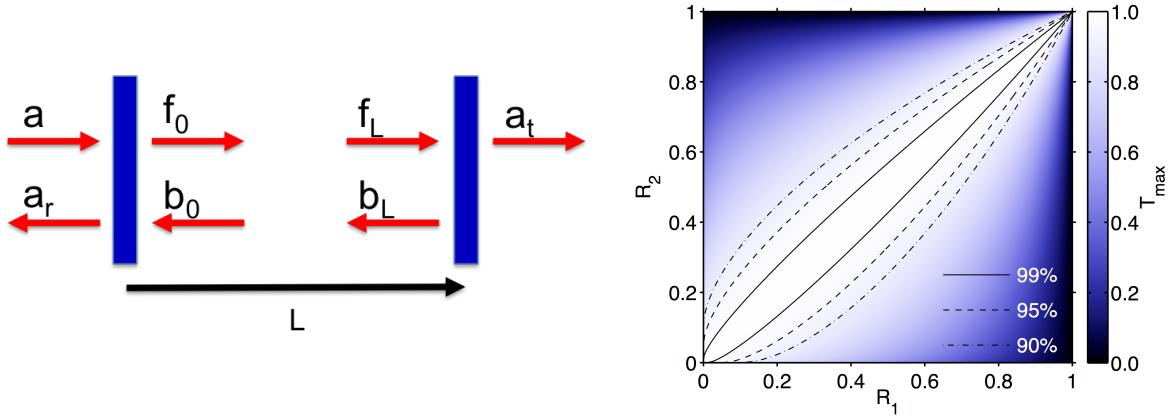

(a) (b)

Figure 4: (a) A Fabry-Perot model with two, not necessarily equal reflectors at a distance L. The complex amplitudes of the incoming and outgoing waves are introduced. (b) Maximal transmittance T_{max} depending of the reflectances R_1 and R_2 of the two reflectors. Even if they are slightly different, the transmittance remains close to 1.

material (here SiO_2) both corners of the step are identical, leading to an ideal Fabry-Perot resonance behavior. But for the asymmetrical case both corners exhibit different reflectances.

In order to get more insight into the asymmetrical step-discontinuity, this system has been modeled as an asymmetric Fabry-Perot resonator as illustrated in Fig. 4(a). The angle of incidence is assumed to be greater than the critical angle θ_{TM}, which means that only the fundamental TE-mode has to be considered. The blue rectangles represent abstract structures, separated by the distance L, at which a part of the light is reflected and the other part is transmitted. Both reflectors exhibit no losses and may be different. Formally one can express this problem in terms of the scattering matrices with reflection coefficients ρ_i and transmission coefficients τ_i that relate the complex amplitudes of the waves:

$$\begin{pmatrix} a_r \\ f_0 \end{pmatrix} = \begin{pmatrix} \rho_1 & \tau_1 \\ \tau_1 & \rho_1 \end{pmatrix} \begin{pmatrix} a \\ b_0 \end{pmatrix}, \qquad \begin{pmatrix} b_L \\ a_t \end{pmatrix} = \begin{pmatrix} \rho_2 & \tau_2 \\ \tau_2 & \rho_2 \end{pmatrix} \begin{pmatrix} f_L \\ 0 \end{pmatrix}, \tag{2}$$

with the relations $f_L = f_0 \cdot \exp(-ik_0 NL)$, $b_L = b_0 \cdot \exp(+ik_0 NL)$, and $|\rho_j|^2 + |\tau_j|^2 = 1$. Here N is the effective index of the wave that passes forth and back between the reflectors. Solving this system of equations for a_r and a_t, which are needed to get the transmittance T and the reflectance R of the whole system, one obtains

$$a_r = \left(\rho_1 + \frac{\tau_1^2 \rho_2}{\exp(i2k_0 nL) - \rho_1 \rho_2}\right) a, \qquad a_t = \left(\frac{\exp(ik_0 nL)\tau_1 \tau_2}{\exp(i2k_0 nL) - \rho_1 \rho_2}\right) a. \tag{3}$$

Transmittance maxima occur for $2k_0NL - \delta = m \cdot 2\pi$, where the phase difference δ is defined by the relation $\rho_1\rho_2 = |\rho_1||\rho_2|\exp(i\delta)$. There the transmittance attains the maximum level

$$T_{max} = \left|\frac{a_t}{a}\right|^2 = \frac{(1-|\rho_1|^2)(1-|\rho_2|^2)}{(1-\rho_1\rho_2)^2}. \tag{4}$$

The maximum transmittance T_{max} is plotted in dependence of the reflectances $|\rho_i|^2$ in Fig. 4(b). Fortunately, such a resonator is forgiving regarding the difference of the reflectances. The solid line indicates the contour, at which the maximum transmittance is still $T_{max} = 99\%$, which already allows a considerable difference of the reflectances.

In order to calculate the distance between two maxima, one has to keep in mind the oblique incidence. The fundamental TE mode mediates between the reflectors, propagating at an angle θ, such that its wavenumber component $k_0 N_{TE}\cos\theta$ in the x-direction becomes relevant for the built up of the resonance. This relates to an effective index $N = N_{TE}\cos\theta$, such that the distance in height ΔL between two consecutive maxima in the transmittance is given by

$$\Delta L = \frac{\lambda_0}{2N_{TE}\cos\theta}. \tag{5}$$

At a vacuum wavelength of $\lambda_0 = 1550nm$ one obtains for a glass covered step $\Delta L_{sym} = 0.63\mu m$ and for an air covered step $\Delta L_{asym} = 0.59\mu m$.

4. SLAB WAVEGUIDE STEPS AT OBLIQUE INCIDENCE

With the goal of maximum power transfer, we select angles of incidence close to the transmittance maxima of the TE modes in Fig. 2 ($\theta = 64°$ for the symmetrical and $\theta = 62°$ for the asymmetrical case). All former arguments on suppression of radiation losses, and on suppression of polarization conversion, rely on the properties of the outgoing slabs only, without any reference to the particular shape of the structure that connects these outlets. We can thus expect, at this angle of incidence, and for identical slab properties, that neither radiation losses nor conversion to TM occur when the step is being excited by the TE_0 wave.

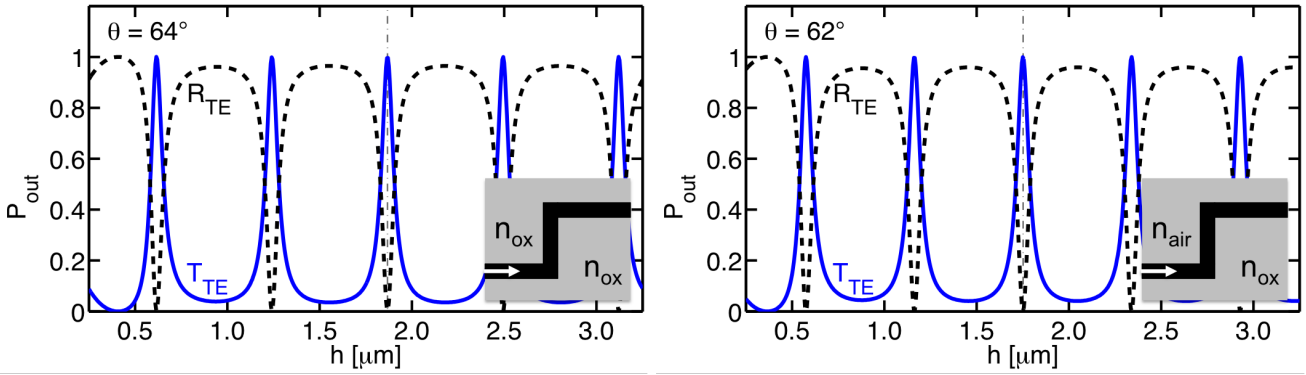

(a) (b)

Figure 5: Transmittance T_{TE} and reflectance R_{TE} as a function of the step height h. In (a) the waveguide is clad with SiO_2 and the angle of incidence is $\theta = 64°$, whereas in (b) the waveguide is covered with air and the angle of incidence is $\theta = 62°$.

In Fig. 5 the transmittance and reflectance as a function of the step height h are shown for the silicon dioxide clad (a) and the air covered case (b). Both exhibit a typical form of a Fabry-Perot resonator, where the distances between the maxima are given by equation 5. Please note that the transmittance and reflectance lines for small heights seem to be deformed. This is the result of the evanescent fields excited by each corner.

In Fig. 6(a) the normalized absolute value $\mathbf{E}$ of the electric field is shown for the non-symmetric step for an angle of incidence of $\theta = 62°$, for a step height of $h = 1.75\mu$m with extremal transmittance. We forgone

the symmetric case, because it looks almost identical to the symmetric case[10] (but note that a different angle of incidence and a different step height is required). For both cases our simulations predict numerical full transmittance of $T > 99\%$. It is not surprising then, that the combination of more such corners can be (almost) arbitrary. As example in Fig. 6(b) a bridge-like structure, with an intermediate upper waveguide segment of, in principle, arbitrary length (here 1.5μm), is shown for the same angle of incidence, also exhibiting a transmittance of $T > 99\%$.

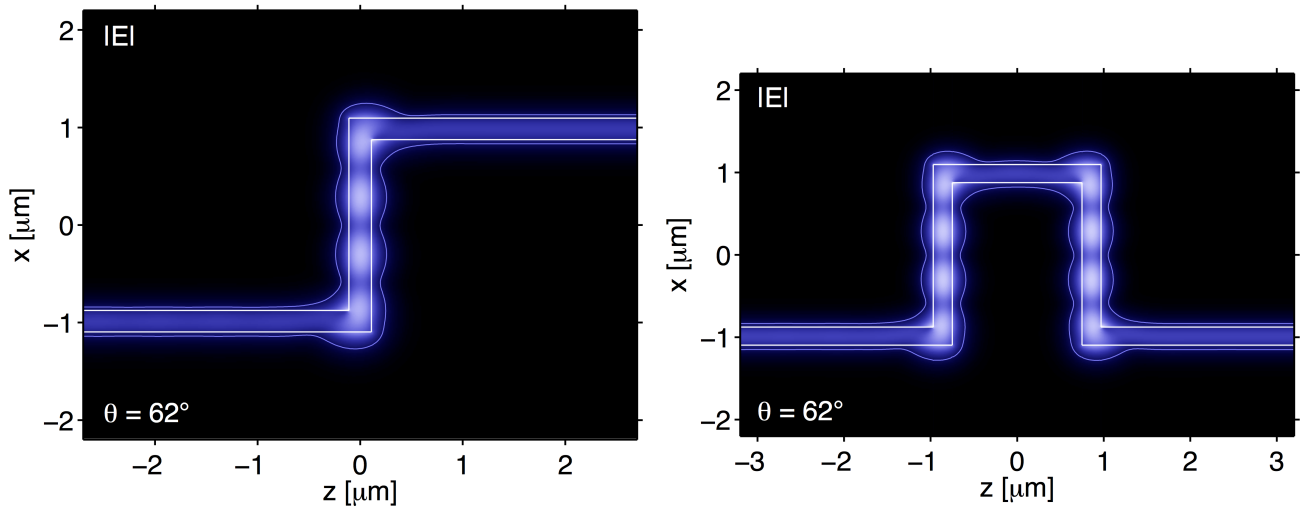

(a) (b)

Figure 6: Field profiles (normalized absolute value $|\mathbf{E}|$ of the electric field, contour at 10% of the field maximum) for (a) the step and (b) a bridge configuration. Both exhibit a transmittance $T > 99\%$.

5. CONCLUDING REMARKS

In conclusion, we have shown that semi-guided planar optical waves *can* be made to climb steps, without radiation losses, polarization conversion, or reflections. This is achieved for simple dielectric slabs, with relatively modest means of oblique incidence, combined with a Fabry-Perot-like resonance effect. For the material system at hand, it is of no importance, if the waveguide is clad by silicon dioxide or not, only the angle of incidence varies slightly. It is apparent, that the step height depends on the angle of incidence, so almost arbitrary heights can be realized, using the right incident angle.

Please note, that the focus of this paper has been the comparison of the symmetric and the asymmetric case of such waveguides as well as the fundamentals. Also interesting is the performance of such a step, if the mode is not infinitely large in lateral direction. In Ref. [11] also Gaussian beams have been investigated leading to lower, but still high transmittances. This has further been confirmed by numerical simulations, solving the full Maxwell's equations using the finite integration technique (FIT).[21] Furthermore it could be shown, that for beam widths larger than 7 μm a transmittance of $T \simeq 80\%$ could be achieved even for smaller angles.[22]

However, there are still a lot of details in need of investigation. Such steps might be improved by rounding the corners, which should increase the general tolerances. The incident angles shown in this paper are rather large, so the region between the critical angles θ_{ox} and θ_{TM}, where radiation losses are still suppressed, could be further analyzed / utilized (c.p. Ref. 11). Additionally, it is worth to transfer this concept to laterally confined waveguides like rectangular waveguides. Apart from that, it would be interesting, to use different material systems, maybe with a lower index contrast.

Acknowledgments

Financial support from the German Research Foundation (Deutsche Forschungsgemeinschaft DFG, projects HA 7314/1-1, GRK 1464, and TRR 142) is gratefully acknowledged.

REFERENCES

[1] Asghari, M. and Krishnamoorthy, A. V., "Silicon photonics: Energy-efficient communication," *Nature photonics* **5**(5), 268–270 (2011).

[2] Prakash Koonath, P. and Jalali, B., "Multilayer 3-D photonics in silicon," *Optics Express* **15**(20), 12686–12691 (2007).

[3] Sherwood-Droz, N. and Lipson, M., "Scalable 3D dense integration of photonics on bulk silicon," *Optics Express* **19**(18), 17758–17765 (2011).

[4] Soref, R. A., Cortesi, E., Namavar, F., and Friedman, L., "Vertically integrated silicon-on-insulator waveguides," *IEEE Photonics Technology Letters* **3**(1), 22–24 (1991).

[5] Doylend, J. K., Knights, A. P., Brooks, C., and Jessop, P. E., "CMOS compatible vertical directional coupler for 3D optical circuits," in [*Proceedings of SPIE*], **5970**, 59700G–10 (2005).

[6] Sun, R., Beals, M., Pomerene, A., Cheng, J., Hong, C.-Y., Kimerling, L., and Michel, J., "Impedance matching vertical optical waveguide couplers for dense high index contrast circuits," *Optics Express* **16**(16), 11682–11690 (2008).

[7] Bauters, J. F., Davenport, M. L., Heck, M. J. R., Doylend, J. K., Chen, A., Fang, A. W., and Bowers, J. E., "Silicon on ultra-low-loss waveguide photonic integration platform," *Optics Express* **21**(1), 544–555 (2013).

[8] Dong, P. and Kirk, A. G., "Compact grating coupler between vertically stacked silicon-on-insulator waveguides," in [*Proceedings of SPIE*], **5357**, 135–142 (2004).

[9] Bessette, J. T. and Ahn, D., "Vertically stacked microring waveguides for coupling between multiple photonic planes," *Optics Express* **21**(11), 13580–13591 (2013).

[10] Hammer, M., Hildebrandt, A., and Förstner, J., "How planar optical waves can be made to climb dielectric steps," *Optics Letters* **40**(16), 3711–3714 (2015).

[11] Hammer, M., Hildebrandt, A., and Förstner, J., "Full resonant transmission of semi-guided planar waves through slab waveguide steps at oblique incidence," *Journal of Lightwave Technology* (2016). in press.

[12] Hammer, M., "Oblique incidence of semi-guided waves on rectangular slab waveguide discontinuities: A vectorial QUEP solver," *Optics Communications* **338**, 447–456 (2015).

[13] Hammer, M., "Quadridirectional eigenmode expansion scheme for 2-D modeling of wave propagation in integrated optics," *Optics Communications* **235**(4–6), 285–303 (2004).

[14] Hammer, M., "METRIC — Mode expansion tools for 2D rectangular integrated optical circuits." http://metric.computational-photonics.eu/.

[15] Peng, S.-T. and Oliner, A., "Guidance and leakage properties of a class of open dielectric waveguides: Part I — mathematical formulations," *IEEE Transactions on Microwave Theory and Techniques* **MTT-29**(9), 843–854 (1981).

[16] Shen, T. P., Wallis, R. F., Maradudin, A. A., and Stegeman, G. I., "Fresnel-like behavior of guided waves," *Journal of the Optical Society of America A* **4**(11), 2120–2132 (1987).

[17] Biehlig, W. and Langbein, U., "Three-dimensional step discontinuities in planar waveguides: Angular-spectrum representation of guided wavefields and generalized matrix-operator formalism," *Optical and Quantum Electronics* **22**(4), 319–333 (1990).

[18] Çivitci, F., Hammer, M., and Hoekstra, H. J. W. M., "Semi-guided plane wave reflection by thin-film transitions for angled incidence," *Optical and Quantum Electronics* **46**(3), 477–490 (2014).

[19] Wagatsuma, K., Sakaki, H., and Saito, S., "Mode conversion and optical filtering of obliquely incident waves in corrugated waveguide filters," *IEEE Journal of Quantum Electronics* **15**(7), 632–637 (1979).

[20] Van Roey, J. and Lagasse, P. E., "Coupled wave analysis of obliquely incident waves in thin film gratings," *Applied Optics* **20**(3), 423–429 (1981).

[21] CST AG, Darmstadt, Germany; http://www.cst.com.

[22] Alhaddad, S., "Propagation planarer, optischer Wellen in Stufenfilmwellenleitern unter schrägem Einfall." master thesis, Paderborn University, 2015.